CHAPTER II

BACKGROUND AND LITERATURE SURVEY

2.1 Natural Gas Storage (Rojey, 1997)

Natural gas storage is necessary for the seasonal adjustment of consumption and gas supply, as a demand for heating is different in winter and in summer. It is used also for balancing daily and hourly fluctuations.

In view of the large specific volume occupied by natural gas at ambient temperature and pressure, its storage is faced with the same difficulties as those encountered in transport. Underground storage in depleted reservoirs, aquifers or salt cavities can be used. Underground storage is used mainly for seasonal load-balancing purposes, although it can cover any fluctuations, whereas liquidfied petroleum gas (LPG) can be performed for short-term adjustment.

Gas storage in depleted reservoirs is the most worldwide and most economical. Storing gas in a depleted reservoir is comparatively simple, because the reservoirs which formerly contained gas or oil, satisfies the permeability, and porosity conditions required for storage. However, before developing a storage facility in a depleted reservoir, it is necessary or ensure that it meets the production targets and that the tightness of the cap rock is satisfactory.

An aquifer-storage facility is illustrated in Figure 2.1. The annual operating cycle of an aquifer-storage facility roughly includes two phases:

- An injection phase during which natural gas is sent to the reservoir by displacing the water in the aquifer.
- A withdrawal phase when the gas is produced at the wellhead and the water reoccupies the pores from which it had been expelled in the injection phase.
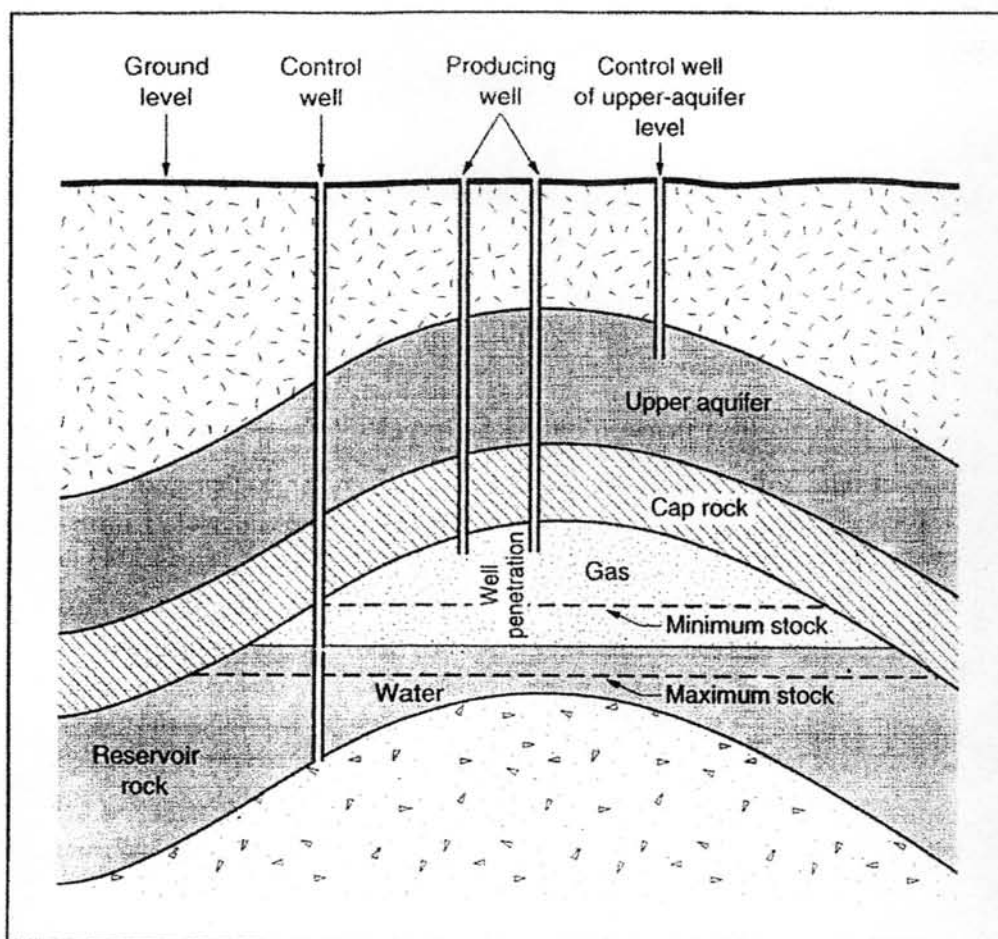
Figure 2.1 Natural gas storage in an aquifer (Rojey, 1997).

The proper operation of an aquifer-storage facility requires that a large quantity of natural gas, called "cushion gas" is maintained in place after withdrawal, to prevent flooding of the producing well, and to allow rapid resumption of the injection phase.

The conditions demanded of aquifers for high-pressure gas storage correspond to those of natural-gas deposits; a good depth of a porous formation, permeable both vertically and horizontally, overlaid by a cap or caps of impermeable rock. A sketch of an aquifer in Iowa, USA is shown in Figure 2.2.
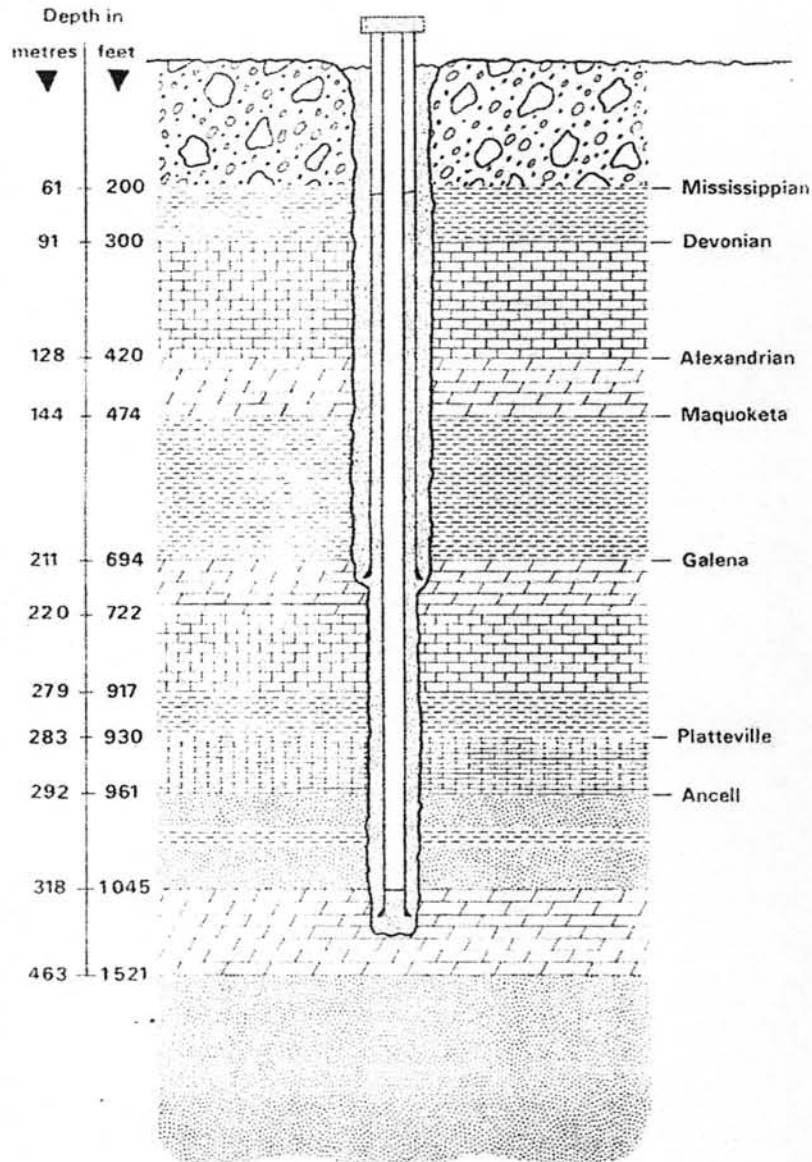
Figure 2.2 Cross-section of a typical aquifer in Iowa, USA (Courtesy of the Institution of Gas Engineers, Edgelow, 1992).

Salt-cavern storage is much more limited in terms of capacity. The salt cavern is obtained by dissolution (leaching) of deep salt beds. The volume of cushion gas required is smaller than in aquifer storage. Salt-cavern storage is used when the regional geological data make aquifer storage unfeasible. It also offers the advantage of delivering a much larger maximum gas flow rate in comparison with the volume stored than an aquifer-storage facility. In an aquifer, viscous friction slows down the flow of the gas in the reservoir rock.

2.2 Reservoir Simulation (Dawe, 2000)

The exploration for natural gas typically begins with geologists examining the surface structure of the earth, and determining areas where it is geologically likely that petroleum or gas deposits might exist. By surveying and mapping the surface and sub-surface characteristics of a certain area, the geologist can extrapolate which areas are most likely to contain a petroleum or natural gas.

The geologist has many information attained from the rock cuttings and samples obtained from the digging of irrigation ditches, water wells, and other oil and gas wells. This information is all combined to allow the geologist to make inferences as to the fluid content, porosity, permeability, age, and formation sequence of the rocks underneath the surface of a particular area.

The data will be analyzed for possible source rocks with a view to determining the degree to which the organic material has been altered by time, heat and pressure, identifying possible petroleum source rocks, and assessing the burial history and petroleum potential of the sediments. Petrophysics comprises the study of physical properties and the fluids contained of rocks. At this stage geologists must work closely with the well log analyst, the reservoir engineers and production engineers. Reservoir simulation implements various numerical techniques by constructing a simulation reservoir for solving such a problem. During simulation steps, it requires inputting of many parameters that are related to the reservoir rocks and fluids as discuss before. This integrated approach ensures that the geological model and the simulation model use the same data interpreted with the best technical competence.

Reservoir simulation is used for evaluating remaining oil and recovery factors under different operation (natural depletion, water/gas injection and production rate), comparison of development schemes for required offtake, evaluating effects of an aquifer on natural water drive, determining the effects of uncertainties in reservoir description of complex reservoirs on development planning and studying the effects of platform location and the spacing of the wells, and, the effects of continuity of pore space and fluids, particularly with horizontal well placements.

Figure 2.3 indicates the information that is input into a simulator and the reservoir simulation process can be divided into following steps:

1. Obtain reservoir data from geophysicist and geologist for gridding; reservoir maps, net to gross maps.

2. Compile the input data for the initialization: porosity, permeability, saturation distribution maps, and fluid distribution.

3. Define reservoir regions and aquifer; continuity, faults, zonation and layering, for coarse/fine grids; set out x-y grid on top surface map; define Δx and Δy dimensions and assign layers and the Δz values, depth of each block in layer.

4. Check the initialization data for errors.

5. Compare gross rock volume, porosity values and compute pore volume.

6. Calculate initial pressure and saturation distributions in reservoir; when the initial data are put into the model. The model is initialized so that saturations and pressure computed throughout the model; check on previous material balance equation for oil in place, gas in place, free gas in place, water in place and pressure. If the static calculations agree, the model is validated; if not, then the input and calculations must be re-checked.

7. Read well data for simulation. For each cell block in the simulator grid system, there must be a value of dimensions for cell and grid blocks, thickness, elevation from fluid contacts, porosity, absolute/effective permeability, rock compressibility, capillary and relative permeability data, pressure-dependent data, thermodynamic data, and viscosity.

8. Initial reservoir pressure, initial phase saturations.

9. Calculate the size of the next time step.

10. Modify computer-calculated transmissibility.

11. Calculate the pressure and saturation distributions at the next time step; solving method and solver are important.

12. Graphical output in color with fluid movements, saturations, pressure.

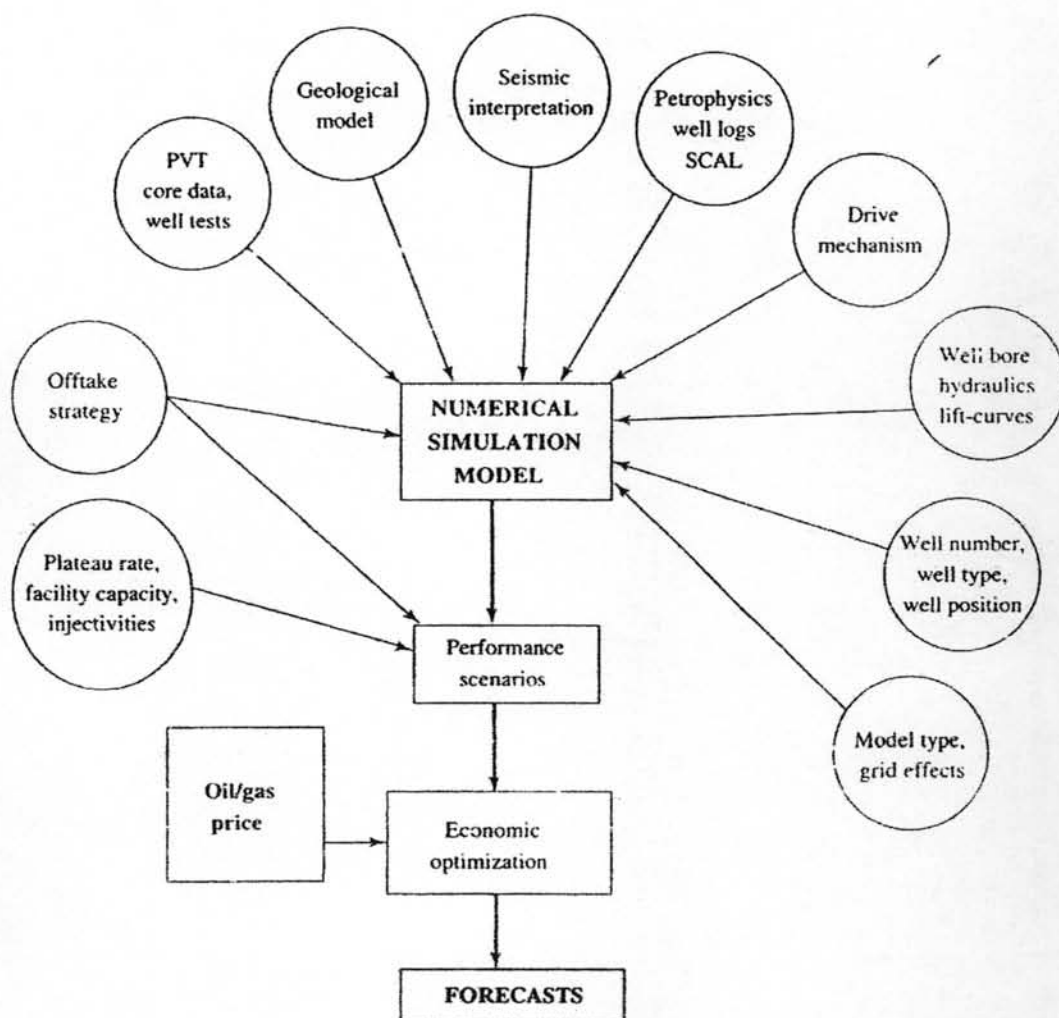13. Compare results with what might be reasonable anticipated.

Figure 2.3 Simulation inputs (Dawe, 2000).

2.3 The Alternating-Direction Implicit (ADI) Scheme in Three Dimensions for the case of square grids ($\Delta x = \Delta y = \Delta z$) (Carnahan, Luther, and Wilkes, 1990)
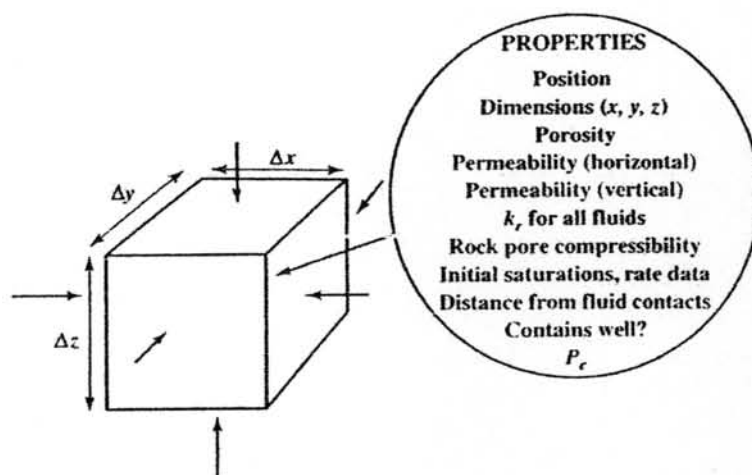

Figure 2.4 Three-dimensional gridblock.

The standard ADI method in three dimensions as defined in Figure 2.4 and Eqs. (2-1) is carried out in three substeps of equal duration $\Delta t/3$, where one spatial dimension is treated implicitly, while the other two dimensions are treated explicitly within each step. The ADI method is:

$$\frac{\partial T}{\partial t} = k\left(\frac{\partial^2 T}{\partial x^2} + \frac{\partial^2 T}{\partial y^2} + \frac{\partial^2 T}{\partial z^2}\right) \tag{2-1}$$

For the first substep from T^l to $T^{l+1/3}$ as expressed in Eqs. (2-2) and (2-3), the equations are implicit in the y and z direction.

$$\frac{T_{i,j,k}^{l+1/3} - T_{i,j,k}^{l}}{\Delta t/3} = k\left[\frac{T_{i+1,j,k}^{l+1/3} - 2T_{i,j,k}^{l+1/3} + T_{i-1,j,k}^{l+1/3}}{(\Delta x)^2} + \frac{T_{i,j+1,k}^{l} - 2T_{i,j,k}^{l} + T_{i,j-1,k}^{l}}{(\Delta y)^2} + \frac{T_{i,j,k+1}^{l} - 2T_{i,j,k}^{l} + T_{i,j,k-1}^{l}}{(\Delta z)^2}\right] \tag{2-2}$$

$$-\lambda T_{i-1,j,k}^{l+1/3} + (3+2\lambda)T_{i,j,k}^{l+1/3} - \lambda T_{i+1,j,k}^{l+1/3} = \begin{pmatrix} \lambda T_{i,j-1,k}^{l} + \lambda T_{i,j+1,k}^{l} + (3-4\lambda)T_{i,j,k}^{l} \\ + \lambda T_{i,j,k-1}^{l} + \lambda T_{i,j,k+1}^{l} \end{pmatrix} \qquad (2\text{-}3)$$

where, $\lambda = \dfrac{k(\Delta t)}{\Delta x^2}$

For the second substep from $T^{l+1/3}$ to $T^{l+2/3}$ as expressed in Eqs. (2-4) and (2-5), the equations are implicit in the x and z direction.

$$\frac{T_{i,j,k}^{l+2/3} - T_{i,j,k}^{l+1/3}}{\Delta t/3} = k \begin{bmatrix} \dfrac{T_{i+1,j,k}^{l+1/3} - 2T_{i,j,k}^{l+1/3} + T_{i-1,j,k}^{l+1/3}}{(\Delta x)^2} + \\[4mm] \dfrac{T_{i,j+1,k}^{l+2/3} - 2T_{i,j,k}^{l+2/3} + T_{i,j-1,k}^{l+2/3}}{(\Delta y)^2} + \\[4mm] \dfrac{T_{i,j,k+1}^{l+1/3} - 2T_{i,j,k}^{l+1/3} + T_{i,j,k-1}^{l+1/3}}{(\Delta z)^2} \end{bmatrix} \qquad (2\text{-}4)$$

$$-\lambda T_{i,j-1,k}^{l+2/3} + (3+2\lambda)T_{i,j,k}^{l+2/3} - \lambda T_{i,j+1,k}^{l+2/3} = \begin{pmatrix} \lambda T_{i-1,j,k}^{l+1/3} + \lambda T_{i+1,j,k}^{l+1/3} + (3-4\lambda)T_{i,j,k}^{l+1/3} \\ + \lambda T_{i,j,k-1}^{l+1/3} + \lambda T_{i,j,k+1}^{l+1/3} \end{pmatrix} \qquad (2\text{-}5)$$

For the third substep from $T^{l+2/3}$ to T^{l+1} as expressed in Éqs. (2-6) and (2-7), the equations are implicit in the x and y direction.

$$\frac{T_{i,j,k}^{l+1} - T_{i,j,k}^{l+2/3}}{\Delta t/3} = k \begin{bmatrix} \dfrac{T_{i+1,j,k}^{l+2/3} - 2T_{i,j,k}^{l+2/3} + T_{i-1,j,k}^{l+2/3}}{(\Delta x)^2} + \\[4mm] \dfrac{T_{i,j+1,k}^{l+2/3} - 2T_{i,j,k}^{l+2/3} + T_{i,j-1,k}^{l+2/3}}{(\Delta y)^2} + \\[4mm] \dfrac{T_{i,j,k+1}^{l+1} - 2T_{i,j,k}^{l+1} + T_{i,j,k-1}^{l+1}}{(\Delta z)^2} \end{bmatrix} \qquad (2\text{-}6)$$

$$-\lambda T_{i,j,k-1}^{l+1} + (3+2\lambda)T_{i,j,k}^{l+1} - \lambda T_{i,j,k+1}^{l+1} = \begin{pmatrix} \lambda T_{i-1,j,k}^{l+2/3} + \lambda T_{i+1,j,k}^{l+2/3} + (3-4\lambda)T_{i,j,k}^{l+2/3} \\ + \lambda T_{i,j-1,k}^{l+2/3} + \lambda T_{i,j+1,k}^{l+2/3} \end{pmatrix} \qquad (2\text{-}7)$$

2.4 Literature Survey

Chamnakyut (2004) studied a simulation of underground storage of natural gas. The numerical simulation program for predicting the pressure profile of natural gas in an underground storage reservoir was developed. The computer program was written for a two-dimensional model and a single layer to solve a governing equation that is a partial differential equation to obtain an approximate solution of the pressure distribution. Pressure profiles were predicted and the amount of gas withdrawn from a reservoir was calculated using the numerical method called the implicit alternating-direction method (IAD) and important input parameters such as permeability, porosity, initial pressure. The program was written to predict regular and irregular shapes of gas reservoirs at constant and inconstant permeability, the pressure distribution and production rate at different time steps.

Assawaphomthada (2005) studied the natural gas reservoir simulation, using two numerical methods, finite difference method (FDM) and finite element method (FEM). Finite difference method uses ADI scheme to discretize the governing equation which the ADI scheme has been implemented in the FORTRAN program. For the finite element method (FEM), the commercial simulation software package called 'FEMLAB' is employed to solve the governing equation. The reservoir model was initially assumed in regular, irregular and actual reservoir shapes. The simulation results are compared with the historical data. The emphasis of the finite element method was placed on investigating the pressure profile in reservoir.

Wu and Pruess (1997) studied a numerical method for simulating non-Newtonian fluid flow and displacement in porous media. The model developed a three-dimensional, fully implicit, integral finite difference simulator for single- and multi-phase flow of non-Newtonian fluids in porous/fractured media. In an effort to demonstrate the three-dimensional modeling capability of the model, a three-dimensional, two-phase flow example is also presented to examine the model results using laboratory and simulation results excision for the three-dimensional problem with Newtonian fluid flow.

Baoyan *et al.* (2003) studied the sequential method for the black-oil reservoir simulation on unstructured grids. This paper presents new results for applying the sequential solution method to the black-oil reservoir simulation with unstructured grids. The fully implicit solution method was successfully applied to reservoir simulation with unstructured grids. However, the complexity of the fully implicit method and the irregularity of the grids are a very complicated structure of linear equation systems (LESs) and in high computational cost to solve them. The sequential method is applied to reduce the size of the LESs by the low implicit degree of this method. These techniques are applied to field-scale models of both saturated and under saturated reservoirs.

Baoyan *et al.* (2004) studied the comparison of solution schemes for black oil reservoir simulations with unstructured grids. This paper presents comparative results of the fully implicit, iterative IMPES, and sequential solution schemes for black oil reservoir simulations with unstructured grids. The comparative results show that the fully implicit scheme is most stable and robust for both reservoirs, but has the highest memory and computational cost, the sequential scheme takes much less memory and computational cost than the folly implicit scheme to reach the same precision for the under saturated reservoirs, when the same iterative control parameters are used; however, for the saturated reservoirs, the sequential scheme must use stricter iterative control parameters to reach the same precision, and the iterative IMPES scheme is not a good choice for the black oil reservoir simulation.

Ridha (2004) used of reservoir simulation to optimize recovery performance. A three-dimensional finite-difference reservoir simulator integrated in an enhanced off recovery (EOR) expert system was used to determine the reservoir management and production strategies to optimize the oil recovery from a carbonate reservoir. After screening the reservoir for an appropriate EOR process on the basis of its properties, it was determined that miscible carbon-dioxide injection is the most suitable process. The management strategies involved studying the different injection techniques to maximize the project profitability. All simulation runs were conducted using permeability fields that have been conditioned with core data taken from wells in the field. This well configuration was shown to yield the best oil recovery compared to other well configurations.

Henderson *et al.* (2005) studied supercritical fluid flow in porous media: modeling and simulation. The supercritical flow in porous materials employed in chromatography, supercritical extraction and petroleum reservoirs. The fluid is constituted of one pure substance and flow behavior is monophasic, highly compressible and isothermal. The porous media is isotropic, possibly heterogeneous with rectangular format. The heterogeneity of porous media is modeled by a simple power law, which describes the relationship between permeability and porosity. The modeling of the hydrodynamic phenomena incorporates the Darcy's law and the mass balance equation. A conservative finite-difference scheme is used to discretize differential equations. The results of the simulation for pressure and mobility of supercritical and liquid propane flowing through porous media are presented. The mobility of fluid flow in porous media depended on the permeability and fluid viscosity of fluid.

Ibrahiem *et al.* (2005) studied analysis of the temperature increase linkes to the power induced by RF source. Four different numerical methods, in particular an implicit method based on the Alternating Direction Implicit technique (ADI), were applied to solve the Bio-Heat Equation (BHE). The tests performed on the latest have showed that the implicit approach is well adapted to solve this type of equations. The rise of temperature in the human head exposed to the RF emission of a mobile phone with a radiated power of 250 mW at 900 MHz was analyzed. The influence of different thermal parameters such as the thermal conductivity and the blood perfusion coefficient on the rise of temperature has been analyzed. The simulation carried out showed that the maximum temperature increase in the internal tissues linked to SAR deposition does not exceed 0.1°C. the record of temperature difference of 1.6°C in the skin due to the presence of a switched off cellular phone, which has been confirmed by the experimental measurements performed.

William and Roland (2002) studied three-dimensional finite element simulation of three-phase flow in a deforming fissured reservoir. The development of a capacity for predicting the exploitation of structurally complicated and fractured oil reservoirs. The mathematical formulation of a three-phase, three-dimensional fluid flow and rock deformation in fractured reservoirs is presented. The presented

formulation consists of both the equilibrium and multiphase mass conservation equations of coupling between the fluid flow and solid deformation, which were usually ignored in the reservoir simulation literature. A Galerkin-based finite element method is applied to discretize the governing equations in space and a finite difference scheme is used to match the solution in time.

Ruben (2004) studied a variational multiscale finite element method for multiphase flow in porous media. A stabilized finite element method for numerical solution of multiphase flow in porous media was based on a multi-scale decomposition of pressures and fluid saturations into resolved (or grid) scales and unresolved (or subgrid) scales. The sub grid problem is modeled using an algebraic approximation. This model requires the definition of a matrix of intrinsic time scales. The performance of the method with simulations of a water flood in a heterogeneous oil reservoir was illustrated. The proposed method yields stable, highly accurate solutions on very coarse grids, which is compared with those obtained by the classical Galerkin method or the upstream finite difference method.